RSC Advances

RSC Advances

www.rsc.org/advances

ROYAL SOCIETY OF CHEMISTRY

www.rsc.org/advances

Journal Name

ARTICLE

Dual enzyme responsive and targeted nanocapsules for intracellular delivery of anticancer agents

Krishna Radhakrishnan†[a], Jasaswini Tripathy†[a,c], Divya P. Gnanadhas[b], Dipshikha Chakravortty[b], Ashok M. Raichur[a].

We report the fabrication of dual enzyme responsive hollow nanocapsules which can be targeted to deliver anticancer agents specifically inside cancer cells. The enzyme responsive elements, integrated in the nanocapsule walls, undergo degradation in the presence of either trypsin or hyaluronidase leading to the release of encapsulated drug molecules. These nanocapsules, which were crosslinked and functionalised with folic acid, showed minimal drug leakage when kept in pH 7.4 PBS buffer, but released the drug molecules at a rapid rate in the presence of either one of the triggering enzymes. Studies on cellular interactions of these nanocapsules revealed that doxorubicin loaded nanocapsules were taken up by cervical cancer cells via folic acid receptor medicated endocytosis. Interestingly the nanocapsules were able to disintegrate inside the cancer cells and release doxorubicin which then migrated into the nucleus to induce cell death. This study indicates that these nanocapsules fabricated from biopolymers can serve as an excellent platform for targeted intracellular drug delivery to cancer cells.

Introduction

Engineered stimuli responsive drug carriers have generated significant interest amongst researchers due to their potential impact on enhancing therapeutic efficacy and safety of pharmaceutical agents. To this end, several drug delivery systems have been reported that respond to a multitude of stimuli which include ultrasound,[1–3] light,[4–7] temperature,[8,9] pH variations[10–12] and redox variations.[13–15] Of these autonomous drug delivery systems responsive to physiological triggers such as pH variations, redox potential and variations in enzyme levels are highly attractive. These systems may be programmed to release drug molecules at suitable locations in the body by utilizing specific physiological cues present there. However, a major complication seen in biologically triggered drug release are the variations in the characteristics of physiological triggers.[16] Although general patterns such as lowering of pH and increase in enzyme levels are commonly seen in some pathological conditions, the quantity and combination of these systems vary from one cell type to another and also between individuals. Hence a generalized approach that utilizes single stimuli to trigger drug release may not work in all situations.

One way to overcome this is to design systems that can respond to multiple stimuli associated with pathological conditions.[17] Some reports of systems that can modulate drug release in response to combinations of stimuli such as pH/temperature,[18–20] pH/ magnetic field,[21,22] temperature/ reduction[23,24] , temperature/ enzyme[25] etc. have been published in the recent years. While most of these systems have been designed to respond to a combination of physiological and non physiological stimuli, very few systems have been reported that can respond to a combination of multiple physiological stimuli. Some of the few examples of systems responsive to multiple physiological stimuli include those that can respond to pH/reduction.[26–28]

An ideal drug carrier has a threefold responsibility. (i) Firstly it has to wholly encapsulate the drug molecule preventing its premature release or degradation (ii) Secondly, the carrier has to carry the drug molecule safely and specifically to the target site (iii) and finally upon reaching the target site, it must release the encapsulated drug molecules by making use of local physiological stimuli present there. In an attempt to design such efficient systems, we have fabricated hollow nanocapsules from biopolymers that are responsive to different enzyme stimuli. The drug molecules can be loaded in the hollow core of the capsules and the stimuli responsive components are integrated in the walls. The walls are crosslinked to minimize premature drug release. This sort of architecture provides a large internal volume that allows very high drug loading compared to matrix architecture. The ratio between the volume

of the wall material and the hollow core is generally very low. Hence a larger amount of drug can be loaded for the same
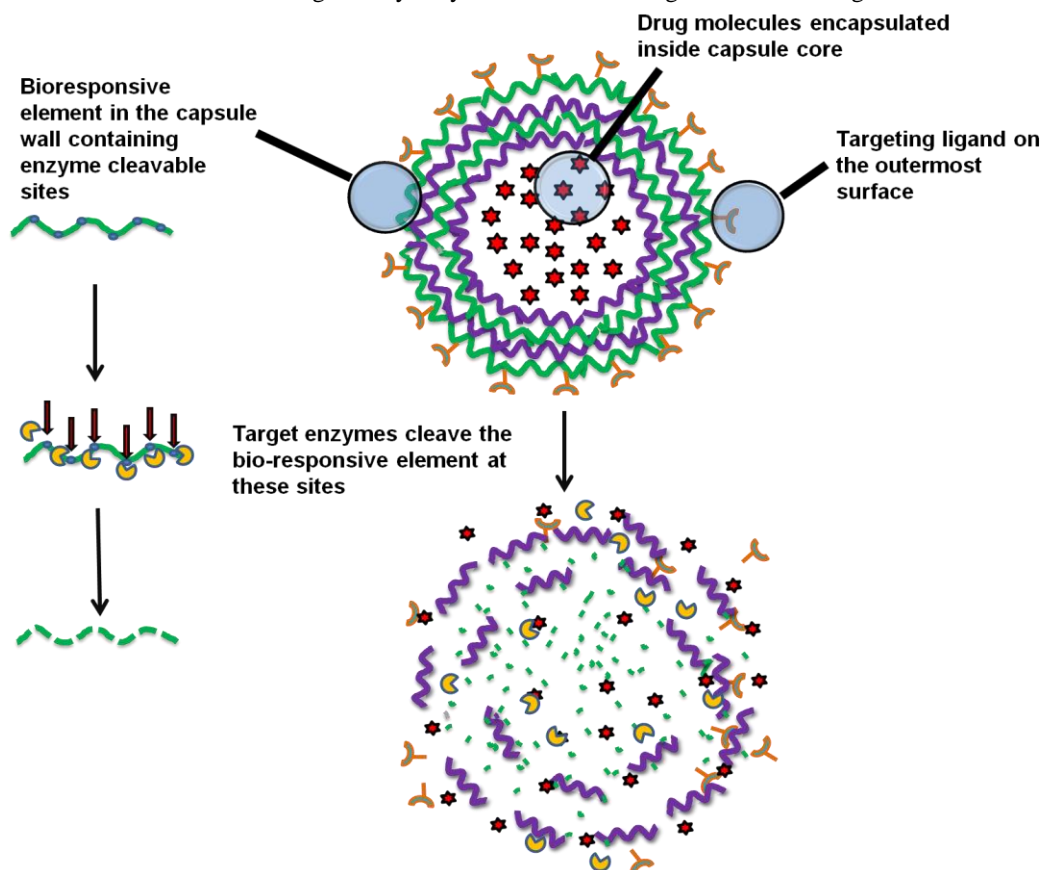
Scheme 1. Schematic representation depicting the design of the nanocapsules

amount of carrier material when compared to solid continuous carrier systems.[29] This type of architecture also allows amplification of the biological stimuli whereby a large number of drug molecules are released in response to subtle biological stimuli. Here a small amount of enzyme can trigger the release of a larger number of drug molecules when compared to other systems such as those based on enzyme responsive prodrugs or solid/matrix nanoparticles.

As stimuli responsive components, polypeptide protamine (PRM) that degrades in the presence of protease enzyme trypsin and the glycosaminoglycan chondroitin sulphate (CS) that degrades in response to endo-β-N-acetlyhexosaminidase such as hyaluronidase were chosen. PRM is a cationic polypeptide that is rich in arginine. It has been used clinically as an FDA approved drug to treat heparin induced toxicity.[30] This molecule is a key constituent in NPH insulin that is administered to diabetes patients to help lower their blood glucose levels. The arginine rich sites in PRM are identified by trypsin and trypsin like proteases that actively cleave these molecules into smaller fragments. Hence it acts as a suitable responsive element for trypsin and trypsin like enzymes. The second stimuli responsive component in the system, chondroitin sulphate has been clinically used in the treatment of arthritis and wound healing. This molecule is susceptible to cleavage by the enzyme hyaluronidase that hydrolyzes 1,4-linkages between 1,4-β-D-glycosidic linkages between N-acetyl galactosamine or N-acetyl-galactosamine sulphate and glucuronic acid. Since

these constituent elements of the nanocapsule are clinically used biopolymers, we expect the system to be biocompatible.

The Layer by Layer (LbL) assembly method was used to fabricate the nanocapsules. LbL fabrication can be carried out under mild conditions and hence offers an excellent platform to incorporate sensitive components such as biopolymers used here.[29] It offers the flexibility to incorporate an array of materials ranging from polypeptides to inorganic nanoparticles. and each functional structure of the capsule has been assembled in a highly controlled manner. Finally, the surface of these Protamine/Chondroitin sulphate (PRM/CHS) nanocapsules was conjugated with a commonly used cancer cell targeting ligand, folic acid. This facilitates the selective uptake of the nanocapsules by folic acid over-expressing cancer cells. We hypothesized that these nanocapsules fabricated from clinically used biopolymers would undergo degradation by utilizing the enzymes present in cancer cells. The intracellular disintegration of nanocapsules followed by release of the encapsulated drug molecules was demonstrated using cervical cancer cell line HeLa cells.

2. Materials and Methods

2.1 Materials.

The polyelectrolytes PRM, CHS, anticancer agent Doxorubicin hydrochloride (FW = 580), 2-(*N*-morpholino)ethanesulfonic

acid (MES), Dulbecco Modified Medium (DMEM) and Fetal calf serum were purchased from Sigma-Aldrich, India. The silica precursor Tetraethoxysilane (TEOS) and Hydrogen fluoride (HF) was obtained from Thomas Baker Ltd. (City, Country) Sodium acetate, Ammonium fluoride (NH_4F), Sodium chloride (NaCl), Sodium Hydroxide (NaOH), Ethanol (C_2H_5OH) and Hydrogen Chloride (HCl) were obtained from Rankem, RFLC Limited (City, Country). Phosphate buffered saline (PBS; 10 X; 137 mM NaCl, 2.7 mM KCl, 10 mM Na_2HPO_4, 1.76 mM KH_2PO_4) obtained from Sigma was diluted 10 times and used for drug release studies. HeLa cells were purchased from National Centre for Cell Science, Pune, India.

2.2. Preparation of nanocapsules

LbL assembly using silica nanoparticles as the template was utilized to fabricate PRM/CHS nanocapsules. Silica nanoparticles were synthesized by modified Stobers method as reported earlier.[12] PRM and CHS were alternatively adsorbed onto the silica at pH 5.6 by incubating silica nanoparticles template in the corresponding polyelectrolyte solution, each having a concentration of 0.5 mg/mL in 0.15M NaCl, for 15 minutes. PRM was the first layer to be adsorbed which was followed by the adsorption of CHS. Each deposition cycle was followed by centrifugation at 2500 rpm for 5 minutes and the residual un-adsorbed polyelectrolyte was removed by washing thrice with pH-adjusted water. After deposition of 3 bilayers, the silica template was removed using 0.2M HF buffered in ammonium fluoride (0.8M; pH 1). The hollow capsules thus obtained were washed with distilled water (pH 5.6) several times.

2.3. Folic acid conjugation

Folic acid conjugation was carried out onto either hollow nanocapsules or capsules with silica core via an EDC/NHS mediated crosslinking reaction. In a typical experiment 1 mg/mL folic acid solution in MES buffer (pH 5.5) was mixed with EDC (0.15 M) and stirred at room temperature for 2 hours. This activated the carboxyl groups of folic acid and resulted in the formation of O-Acyl-isourea intermediates. Activated folic acid solution was added to nanocapsule suspension and kept under constant stirring for 4 hours at ambient temperature. The resulting nanocapsules were purified by ultracentrifugation and intermittent washing with double-distilled water to eliminate un-reacted reactants such as folic acid.

2.4. Zeta potential measurements

The LbL assembly of oppositely charged PRM and CHS on silica templates was followed by measuring the zeta potential after each adsorption cycle using Zetasizer Nano ZS (Malvern, Southborough, MA). The zeta potential values were calculated using the Smoluchowski relation between the ionic mobility and the surface charge of the particles. Each value noted was the average of three repeated measurements performed at pH 5.6.

2.5. Characterization of nanocapsules

Electron microscopy was utilized to study the morphological characteristics of the prepared nanocapsules. The samples were deposited on silicon wafer and air dried followed by sputter-coating with gold (JEOL JFC 1100E Ion sputtering device) and observed in secondary electron imaging mode using field emission – SEM (FEI-SIRION, Eindhoven, The Netherlands). Transmission electron microscopy (TEM) images were taken by using Tecnai F-30 (FEI, Eindhoven, The Netherlands), equipped with a Schottky Field Emission source. The samples were dropcasted onto a copper grid and dried before imaging. The FTIR spectra of the samples were recorded in the range 400 cm^{-1} to 4000 cm^{-1} with a resolution of 4 cm^{-1} using FTIR Bruker, Germany.

2.6 Drug loading and release studies

Capsule suspension was centrifuged at 2500 rpm for 6 minutes and the supernatant was removed. Drug loading was carried out at pH 8 by incubating 100 μL of capsule suspension with 200 μL of doxorubicin having a concentration of 1mg/mL. After 12 hours the drug loaded capsules were centrifuged and supernatant was discarded. The percentage of drug loading was determined by measuring the amount of drug remaining in the supernatant solution after loading. The drug loaded capsules were washed thrice with water of pH 5.6 to remove unabsorbed drug molecules.

100 μL of drug loaded nanocapsules were incubated in 1ml of release media. The release media was either a solution containing Trypsin (100 μg/mL) or a solution containing Hyaluronidase I (500 mU/mL) in pH 6 MES buffer. As a control, pH 7.4 PBS buffer was used to understand the release pattern from the capsules in the absence of the enzyme triggers under physiological pH conditions. Aliquots from the release media were taken at various time points to quantify the drug release. The drug release was calculated by absorbance spectroscopy at 496 nm using a spectrophotometer (ND1000, Nanodrop, USA).

2.7. Cell culture

HeLa cells were cultured in Dulbecco's Modified Medium (DMEM) supplemented with 10% Fetal Calf Serum and penicillin (100 U mL^{-1}). The cells were maintained at 37ºC with 5% CO_2.

2.8. Cellular uptake and intracellular degradation of nanocapsules by CLSM

HeLa cells were seeded on sterile coverslips at a density of 1×10^5 to 2×10^5 and kept in 24 well plates. The cells were allowed to attach and flatten on the coverslip by incubating for 12 h. This was followed by washing the cells three times with PBS. Subsequently the doxorubicin loaded f-PRM/CHS nanocapsules were suspended in the culture media and incubated with these cells. After the required incubation period the cells were washed with PBS and then fixed using 4% paraformaldehyde. The cells were stained with DAPI (4',6-diamidino-2-phenylindole) at a final concentration of 0.5 μg/ml in H_2O. The treated cells were then visualized under a Carl Zeiss CLSM system equipped with a 100x oil immersion objective with a numerical aperture of 1.4. Doxorubicin was excited at 496 nm producing a red colour fluorescence while DAPI excited at 350 nm produced a blue colour fluorescence.

2.9. Flow cytometry analysis

Uptake of the capsules by HeLa cells were analysed by flow cytometry. Briefly, HeLa cells were seeded at a density of 1×10^5 to 2×10^5 in 24 well plates. For folic acid blocking experiment, cells in 24 well plates were firstly treated with 200 µg mL^{-1} folic acid in DMEM medium / only DMEM for 30 min. After washing the cells with PBS, doxorubicin loaded f-PRM/CHS nanocapsules / free doxorubicin suspended in the culture media were incubated with these cells for 6 h. The cells were washed with PBS, scraped and collected by centrifugation (2,000 x *g* for 10 min at 4°C) and then fixed using 4% paraformaldehyde. The cells were subjected to flow cytometric analysis (BD FACSCanto II) and the data were analyzed with WinMDI 2.9.

2.5 Cell viability Assay

Cell viability was assessed using an MTT assay. The HeLa cells were seeded onto a 96 well plate at a density of 5 X 10^4 cells/ mL. Once these cells attached and flattened onto the well plate, different concentrations of the various nanocapsules were added and incubated for 24 hours. After the required incubation time, 20µl of MTT dye, a soluble yellow tetrazolium salt (5mg/ml), was added to each well and kept for another 4 h at 37ºC. The resulting formazan crystals were then solubilized using a buffer (27mL isopropanol, 3mL tritonXV100, 2.5uL HCl). The absorbance (at 570 nm) of the resulting solution was measured and the cell viability was calculated by taking the untreated cells as the control.

3. Results and Discussion

3.1. Fabrication of PRM/CHS hollow nanocapsules

A hollow nanocapsule based drug delivery system was designed that can retain drug molecules at the physiological pH of 7.4, selectively accumulate in tumour cells and by utilizing the microenvironment there, undergoes degradation to bring about drug release. PRM and CHS were assembled on to a sacrificial silica nanoparticle template. The assembly pH was optimized to 5.6 where minimum particle aggregation and efficient layer formation was observed. Formation of LbL assembled multilayers on silica template was monitored by measuring the ζ- potential of the particles after adsorption of each layer adsorption. As given in **Figure 1**. the ζ-potential of the coated silica template alternated between positive and negative values depending on the outermost layer adsorbed. A positive ζ-potential was observed when the outermost layer was protamine whereas particles with chondroitin sulphate as the outermost layer showed a negative ζ-potential.
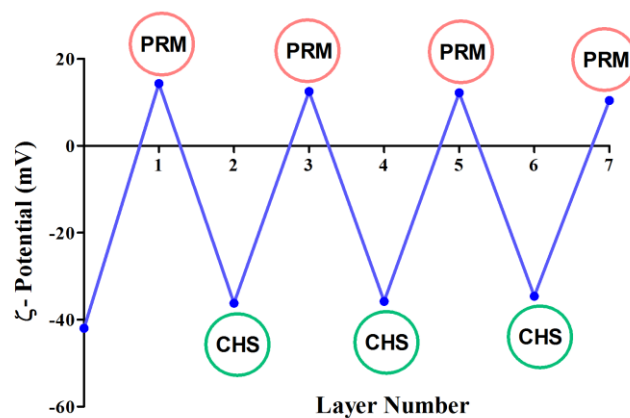
Figure 1. ζ- potential variation as a function of outermost adsorbed layer. It can be seen that CHS as outermost layer gave a negative ζ- potential whereas PRM as in the outermost layer gave positive ζ- potential value.

Upon assembling the required number of multilayers (6 layers), the template was removed by HF treatment. The outermost layer in the assembly was kept as PRM which provided amine groups for folic acid functionalisation. Folic acid conjugation was then carried out by using carbodiimide mediated crosslinking chemistry. In this reaction, the carboxyl groups of folic acid was first activated by treatment with EDC. This resulted in the formation of active O-acylisourea intermediate that readily reacts with the amine groups present in PRM forming an amide bond. The synthesized folic acid conjugated PRM/CHS (f-PRM/CHS) nanocapsules were then visualized using electron microscopy techniques. TEM and SEM images of these nanocapsules are shown in **Figure 2**. The images revealed that the nanocapsules were fairly well dispersed and had a spherical morphology.
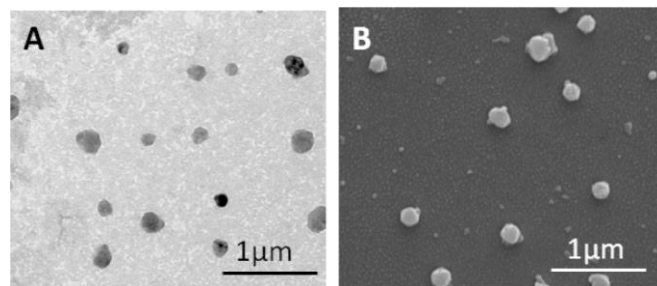
Figure 2. TEM (a) and SEM (b) of f-PRM/CHS nanocapsules

Dynamic Light Scattering (DLS) experiments (**Figure 3.)** showed that the particles had a narrow size distribution with an average hydrodynamic diameter of around 201.8 nm. This is in agreement with the sizes observed in the SEM and TEM micrographs. Folic acid conjugation was confirmed using FTIR spectroscopy (**Figure 4.)** which shows the FT-IR spectra of f-PRM/CHS nanocapsules, free FA and PRM/CHS nanocapsules respectively.
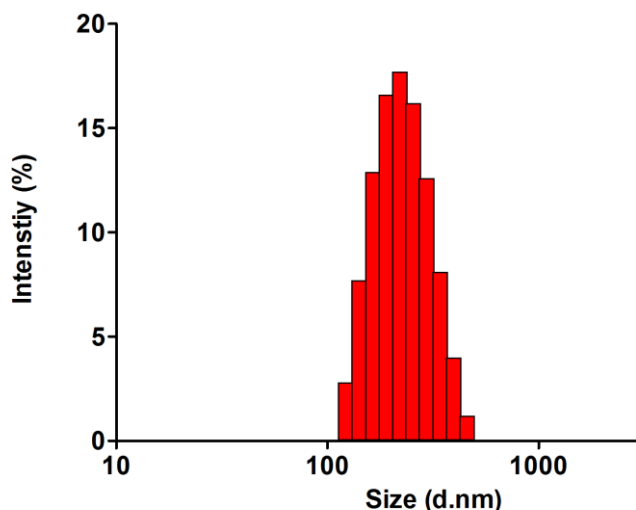
Figure 3. DLS spectra of f-PRM/CHS nanocapsules.

The IR spectrum of free FA depicts characteristic peaks at 1710 cm $^{-1}$ and 1605 cm $^{-1}$ due to the COOH group and the benzene ring of FA. Compared to PRM/CHS, the f-PRM/CHS nanocapsules spectrum exhibited a characteristic absorption peak at 1606 cm^{-1} corresponding to the benzene ring of FA, while the peak at 1650 cm^{-1} corresponds to –CONH amide band. These results are indicative of successful functionalisation of FA onto nanocapsules
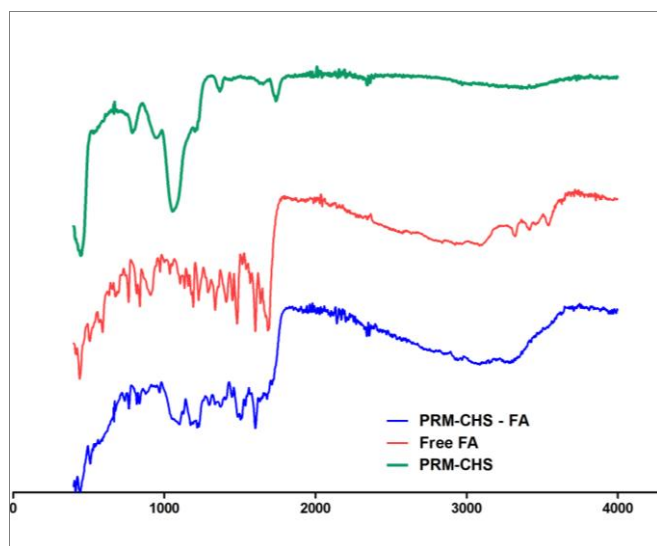

Figure 4. FTIR spectra of f-PRM/CHS nanocapsules, free folic acid, bare nanocapsules. The Y axis of the graphs have been shifted for better visibility.

3.2. Drug loading into f-PRM/CHS nanocapsules

In order to study the enzyme responsive drug release from f-PRM/CHS nanocapsules, an anticancer drug doxorubicin was used as the model drug. Doxorubicin was chosen due to its well characterized absorbance properties and ease of quantification.

Initially, the doxorubicin loading step was carried out after the folic acid conjugation. But it was observed that this resulted in significantly lower drug uptake by the f-PRM/CHS nanocapsules. A possible explanation to this behaviour is the fact that the EDC mediated amide bond formation would not only result in the conjugation of folic acid, but this reaction could also crosslink the carboxyl group of CHS and the amine group of PRM present in the capsule wall resulting in reduction of wall permeability.

In order to overcome this limitation, we loaded doxorubicin into the PRM/CHS nanocapsule core before the folic acid conjugation step. Doxorubicin loading was carried out at pH 8. At this pH the electrostatic interaction between CHS and PRM is minimal and hence the walls are more permeable. Thus we observed an enhanced drug loading of 48 % as compared to the 18% percentage observed after crosslinking. Moreover, doxorubicin attains a positive charge at this pH which is below its pka. Due to this it is attracted to the negatively charged core of the nanocapsules.

3.3. Dual enzyme responsive release behaviour of f-PRM/CHS nanocapsules

In the present work nanocapsule walls have been incorporated with the trypsin responsive PRM and hyaluronidase responsive CHS. Due to this, these nanocapsules were expected to undergo wall degradation initiating drug release in the presence of either of these enzymes as stimuli. In order to evaluate this, we incubated doxorubicin loaded f-PRM/CHS nanocapsules in presence of either trypsin or hyaluronidase. As a control experiment we studied drug release from f-PRM/CHS nanocapsules incubated in PBS buffer (pH 7.4). The PBS buffer (pH 7.4) was chosen as a control as this is the physiological pH of the blood to which the f-PRM/CHS nanocapsules would be exposed to before reaching the target site. As evidenced from the release curve shown in **Figure 5.**, the drug release was minimal from the nanocapsules incubated in PBS.

Interestingly, only 16% of the loaded doxorubicin was released into the PBS even after 12 hours. This suggests that the rate of drug release in the absence of either of the triggering enzymes is negligible and hence chances of premature drug leakage from this system during its transit in the blood stream may be minimal. These phenomena may be explained using two contributing mechanisms: (i) the folic acid conjugation using carbodiimide mediated reactions has resulted in crosslinking between PRM and CHS chains. This results in the formation of compact layers having a very low permeability. (ii) Secondly, the remaining amine functional groups of PRM and carboxyl groups of CHS that has not undergone crosslinking reaction are in the highly protonated state at pH 7.4. This results in strong electrostatic interaction between the layers again contributing to the reduction of capsule wall permeability.

In contrast to this the drug release was greatly enhanced when the f-PRM/CHS nanocapsules were kept in media containing either trypsin or hyaluronidase. The enzyme containing release media was maintained at a slightly acidic pH of 6 to mimic the intracellular microenvironment especially inside the lysosomal compartments. A near burst release was observed from the capsules incubated in the media containing trypsin, with nearly 61% of the loaded doxorubicin getting released in 4 hours. The release was relatively slower after this point reaching nearly 75 % in 12 hours. Similarly, when the nanocapsules were incubated in the presence of hyaluronidase l,

there was an immediate increase in the rate of drug release with 38% of the loaded drug releasing in 4 hours and 54 % in 12 hours.
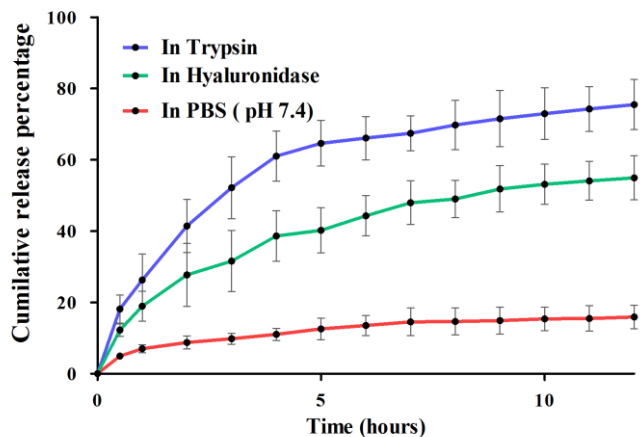

Figure 5. Drug release from f-PRM/CHS nanocapsules incubated with either trypsin, hyaluronidase I or PBS buffer.

As explained above hollow nanocapsule architecture favours fast enzyme mediated release on triggering. The enzymes act on the stimuli responsive components present on the walls and cleave these molecules at various recognized cleavage sites. This results in degradation of the nanocapsule walls slowly increasing the permeability and resulting in drug release. It is worth noting that the rate of drug release from the capsules varied depending on the enzyme trigger employed. Nanocapsules incubated with trypsin (10 μg/mL) was able to release doxorubicin at a faster rate when compared to those incubated with hyaluronidase l (500 mU/mL).

3.4. Cellular uptake and intracellular drug release from f-PRM/CHS nanocapsules

Studies were carried out to understand the fate of these nanocapsules when incubated with cancer cells. Here too we have utilized doxorubicin as a model drug and reporter molecule. Doxorubicin is self fluorescent and hence can be visualized inside cancer cells by CLSM. The doxorubicin loaded f-PRM/CHS nanocapsules were incubated with cervical cancer cells (HeLa cell line) and CLSM images were taken at various time points as shown in **Figure 6**. The blue colour fluorescence appearing in the images is due to the DAPI dye that stains the nucleus of the HeLa cells. It can be observed that within 1 hour of incubation, a red coloured fluorescence was seen localized around the cell membrane of the cancer cells. This can be attributed to the attachment of the doxorubicin loaded PRM/CHS nanocapsules onto the folic acid receptors (FR) present on the cell membrane. HeLa cells are known to over express folic acid receptors that aid them in accumulating nutrients for promoting growth. The folic acid molecules present on the f-PRM/CHS nanocapsules recognize these receptors. This binding later results in internalisation of these nanocapsules as seen from the CLSM image taken after 6 hours incubation. The image in **Figure 6.** shows that the red fluorescence of doxorubicin has spread inside most of the cancer cells. It is worth noting here that the fluorescence coming from the nucleus is predominantly blue although some

of the cells show traces of red that appears pink in the merged images. But the images taken after 12 hours show that the red colour fluorescence of doxorubicin has localized into the nucleus of the cells. This differential localisation of doxorubicin fluorescence is a good indication that the doxorubicin encapsulated inside the nanocapsules are released in a controlled manner. It is generally observed that free doxorubicin when incubated with cancer cells directly migrates into the nucleus within the first 60 minutes. Earlier reports have shown that doxorubicin encapsulated inside nanoparticles remain in the cytoplasm and once these molecules are released from the carrier nanoparticles, they migrate into the nucleus. Hence these results indicate that the doxorubicin present within the nanocapsules have been released subsequent to cellular internalisation.
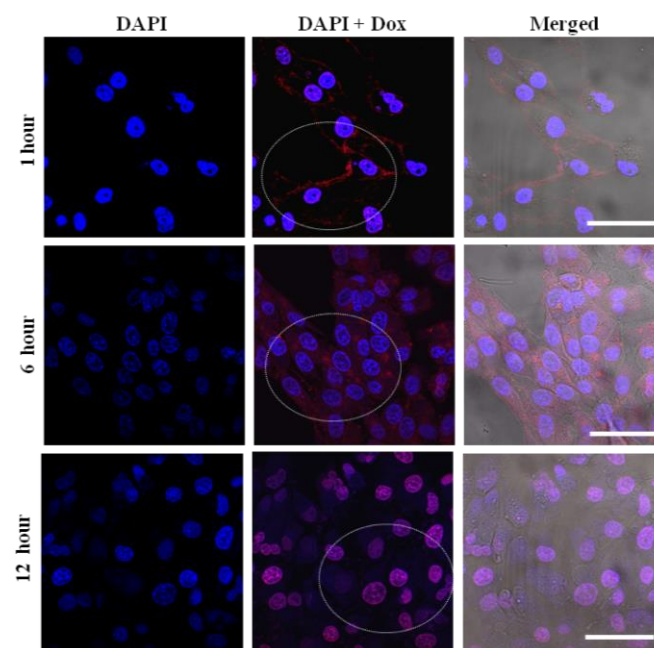

Figure 6. CLSM images of HeLa cells incubated with f-PRM/CHS nanocapsules for various time periods. The blue colour fluorescence is due to the DAPI stain that stains the nucleus whereas the red colour is contributed by the doxorubicin drug. It can be seen from these images that the doxorubicin inside the nanocapsules are released and this has migrated into the nucleus after 12 hours.

3.5. Evaluation of anticancer activity of doxorubicin loaded f-PRM/CHS nanocapsules

Doxorubicin loaded f-PRM/CHS nanocapsules were incubated at various doxorubicin concentrations with a fixed number of HeLa cells. The anticancer activity was measured using an MTT assay which indicated the percentage of cancer cells that have lost viability after treatment with the particular concentration of sample. In order to evaluate the effect of folic acid conjugation on the anticancer activity of encapsulated doxorubicin, non functionalized doxorubicin loaded PRM/CHS nanocapsules were incubated with HeLa cells. As controls, the same number of HeLa cells was treated with at least the same quantity of free doxorubicin; unloaded f-PRM/CHS nanocapsules or unloaded PRM/CHS nanocapsules as present

in doxorubicin loaded f-PRM/CHS nanocapsules. As expected,   the doxorubicin encapsulated inside folic acid conjugated
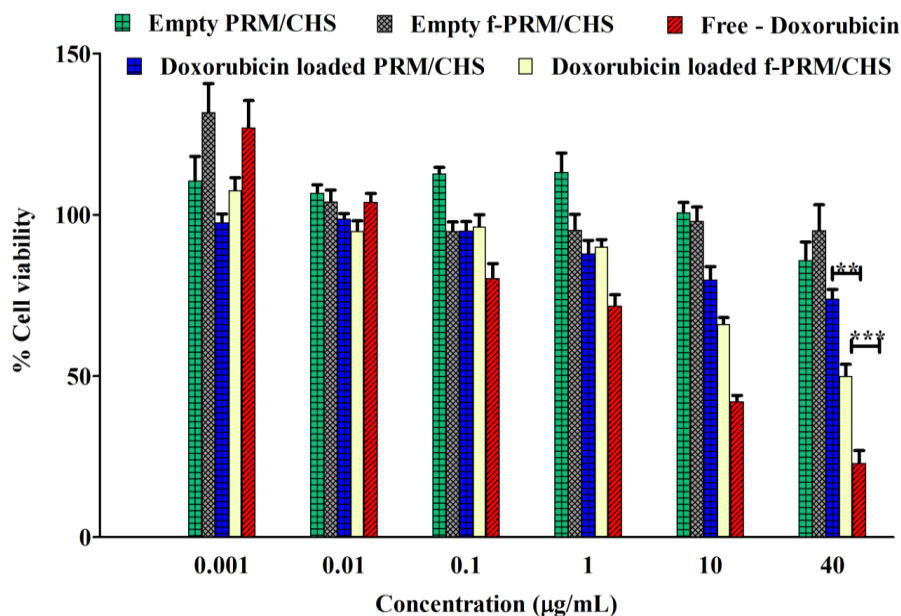

Figure 7. Results of MTT assay using empty or doxorubicin loaded PRM/CHS, f-PRM/CHS nanocapsules and free doxorubicin.

nanocapsules showed enhancement in the anticancer activity as compared to doxorubicin in PRM/CHS nanocapsules. This point towards the fact that FR mediated enhanced cellular uptake of f-PRM/CHS nanocapsules can enhance the cell death of FR +ve cancer cells. It was observed that the anticancer activity of doxorubicin loaded inside the nanocapsules was lower when compared to free doxorubicin (**Figure 7**). This can be attributed to the more efficient uptake of the smaller free drug molecules as compared to the bulky nanocapsules. Moreover, there is a delay in the availability of free doxorubicin from the nanocapsules due to the time required for cellular uptake of nanocapsules, intracellular degradation and gradual release of free doxorubicin.

3.6. Quantification of cellular uptake of nanocapsules

In order to substantiate the MTT results and to demonstrate the effect of folic acid conjugation on cellular uptake of f-PRM/CHS nanocapsules by HeLa cells, a series of experiments were carried out utilizing flow cytometry. f-PRM/CHS nanocapsules were incubated with HeLa cells for 6 h with or without blocking with folic acid prior to the incubation for 30 min. Around 99% of the cells were showing positive for doxorubicin uptake when the PRM/CHS nanocapsules were conjugated with folic acid whereas only 75% of the cells showed positive for doxorubicin uptake when incubated with bare PRM/CHS nanocapsules as depicted in **Figure 8**. This indicated that the folic acid conjugation significantly enhanced cellular uptake of nanocapsules ($P < 0.05$). To confirm the folic acid mediated entry, the cells were pre-treated with folic acid for 30 min to block the folic acid receptor. It was observed that free folic acid blocking of folic acid receptors resulted in a significant decrease ($P < 0.05$) in the cellular uptake of f-PRM/CHS nanocapsules which indicated that partial entry into the cells by the particles is receptor mediated (**Figure 8**).

Interestingly, the folic acid blocking had no effect on the uptake of free doxorubicin (**Figure 8.**).
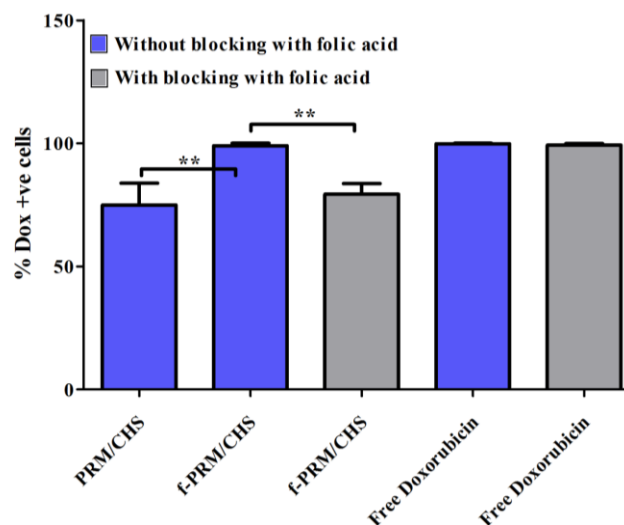
Figure 8. Results of the FACS analysis for comparing cellular uptake of doxorubicin loaded nanocapsules with/without folic acid functionalisation. Effect of blocking folic acid receptors on the cellular uptake of free/ f-PR/CS nanocapsule encapsulated doxorubicin was also studied.

4. Conclusions

The f-PRM/CHS nanocapsules, incorporated with both PRM and CHS, showed controlled drug release in the presence of either trypsin or hyaluronidase. These nanocapsules conjugated with folic acid accumulated inside cancer cells and underwent degradation intracellularly releasing the encapsulated doxorubicin. Anticancer activity of doxorubicin encapsulated inside nanocapsules improved after folic acid molecules were

attached to the nanocapsule surface. These characteristics hold great promise for the development of dual responsive and intracellularly degradable drug delivery systems.

Acknowledgements

Notes and References

† These authors contributed equally.

a Department of Materials Engineering, Indian Institute of Science, Bangalore, 560012, India,
Fax: +91 80 23600472, Tel: +91 80 22933238
Email: amr@materials.iisc.ernet.in
b Department of Microbiology and Cell Biology, Indian Institute of Science, Bangalore, 560012, India,
c School of Applied sciences (Chemistry), KIIT University, Bhubaneswar 751024, Odisha, India

References

1. B. Geers, H. Dewitte, S. C. De Smedt, and I. Lentacker, *J. Controlled Release*, 2012, **164**, 248–255.
2. H.-J. Kim, H. Matsuda, H. Zhou, and I. Honma, *Adv. Mater.*, 2006, **18**, 3083–3088.
3. W. G. Pitt, G. A. Husseini, and B. J. Staples, *Expert Opin. Drug Deliv.*, 2004, **1**, 37–56.
4. C. Alvarez-Lorenzo, L. Bromberg, and A. Concheiro, *Photochem. Photobiol.*, 2009, **85**, 848–860.
5. A. S. Angelatos, B. Radt, and F. Caruso, *J. Phys. Chem. B*, 2005, **109**, 3071–3076.
6. X. Yang, X. Liu, Z. Liu, F. Pu, J. Ren, and X. Qu, *Adv. Mater.*, 2012, **24**, 2890–2895.
7. R. Kurapati and A. M. Raichur, *Chem. Commun.*, 2012, **49**, 734–736.
8. E. Aznar, L. Mondragón, J. V. Ros-Lis, F. Sancenón, M. D. Marcos, R. Martínez-Máñez, J. Soto, E. Pérez-Payá, and P. Amorós, *Angew. Chem. Int. Ed.*, 2011, **50**, 11172–11175.
9. C. Gao, S. Leporatti, S. Moya, E. Donath, and H. Möhwald, *Chem. – Eur. J.*, 2003, **9**, 915–920.
10. L. Chen, J. Di, C. Cao, Y. Zhao, Y. Ma, J. Luo, Y. Wen, W. Song, Y. Song, and L. Jiang, *Chem. Commun.*, 2011, **47**, 2850–2852.
11. K. E. Broaders, S. J. Pastine, S. Grandhe, and J. M. J. Fréchet, *Chem. Commun.*, 2010, **47**, 665–667.
12. A. Raichur, Thomas, Radhakrishnan, Gnanadhas, and D. Chakravortty, *Int. J. Nanomedicine*, 2013, 267.
13. Dai Hai Nguyen, Jong Hoon Choi, Yoon Ki Joung, and Ki Dong Park, *J. Bioact. Compat. Polym.*, 2011, **26**, 287–300.
14. Z. Luo, K. Cai, Y. Hu, L. Zhao, P. Liu, L. Duan, and W. Yang, *Angew. Chem. Int. Ed.*, 2011, **50**, 640–643.
15. C. Zheng, X. G. Zhang, L. Sun, Z. P. Zhang, and C. X. Li, *J. Mater. Sci. Mater. Med.*, 2013, **24**, 931–939.
16. K. Liang, G. K. Such, Z. Zhu, S. J. Dodds, A. P. R. Johnston, J. Cui, H. Ejima, and F. Caruso, *ACS Nano*, 2012, **6**, 10186–10194.
17. R. Cheng, F. Meng, C. Deng, H.-A. Klok, and Z. Zhong, *Biomaterials*, 2013.
18. Y.-C. Chen, L.-C. Liao, P.-L. Lu, C.-L. Lo, H.-C. Tsai, C.-Y. Huang, K.-C. Wei, T.-C. Yen, and G.-H. Hsiue, *Biomaterials*, 2012, **33**, 4576–4588.
19. K. S. Soppimath, D. C.-W. Tan, and Y.-Y. Yang, *Adv. Mater.*, 2005, **17**, 318–323.
20. L. Zhang, R. Guo, M. Yang, X. Jiang, and B. Liu, *Adv. Mater.*, 2007, **19**, 2988–2992.
21. A. Curcio, R. Marotta, A. Riedinger, D. Palumberi, A. Falqui, and T. Pellegrino, *Chem. Commun.*, 2012, **48**, 2400–2402.
22. S. Yu, G. Wu, X. Gu, J. Wang, Y. Wang, H. Gao, and J. Ma, *Colloids Surf. B Biointerfaces*, 2013, **103**, 15–22.
23. R. Cheng, F. Meng, S. Ma, H. Xu, H. Liu, X. Jing, and Z. Zhong, *J. Mater. Chem.*, 2011, **21**, 19013–19020.
24. Y.-Z. You, C.-Y. Hong, and C.-Y. Pan, *Macromolecules*, 2009, **42**, 573–575.
25. C. Chen, J. Geng, F. Pu, X. Yang, J. Ren, and X. Qu, *Angew. Chem. Int. Ed.*, 2011, **50**, 882–886.
26. Y.-J. Pan, Y.-Y. Chen, D.-R. Wang, C. Wei, J. Guo, D.-R. Lu, C.-C. Chu, and C.-C. Wang, *Biomaterials*, 2012, **33**, 6570–6579.
27. W. Chen, P. Zhong, F. Meng, R. Cheng, C. Deng, J. Feijen, and Z. Zhong, *J. Controlled Release*, 2013, **169**, 171–179.
28. S. Shu, X. Zhang, Z. Wu, Z. Wang, and C. Li, *Biomaterials*, 2010, **31**, 6039–6049.
29. C. S. Peyratout and L. Dähne, *Angew. Chem. Int. Ed.*, 2004, **43**, 3762–3783.
30. A. S. Arbab, G. T. Yocum, H. Kalish, E. K. Jordan, S. A. Anderson, A. Y. Khakoo, E. J. Read, and J. A. Frank, *Blood*, 2004, **104**, 1217–1223.

.

RSC Advances Accepted Manuscript